LBL-28737
UC-201

Lawrence Berkeley Laboratory

UNIVERSITY OF CALIFORNIA

Energy Conversion & Storage Program

1989 Annual Report

Applied Science Division

June 1990

LOAN COPY
Circulates
for 2 weeks
Bldg. 50 Library.
LBL-28737
Copy 2

Available to DOE and DOE Contractors from
Office of Scientific and Technical Information
P.O. Box 62, Oak Ridge, TN 37831
Prices available from (615) 576-8401, FTS 626-8401

Available to the public from
National Technical Information Service
U.S. Department of Commerce
5285 Port Royal Road, Springfield, VA 22161

Prepared for the U.S. Department of Energy under Contract No. DE-AC03-76SF00098

DISCLAIMER

This document was prepared as an account of work sponsored by the United States Government. While this document is believed to contain correct information, neither the United States Government nor any agency thereof, nor the Regents of the University of California, nor any of their employees, makes any warranty, express or implied, or assumes any legal responsibility for the accuracy, completeness, or usefulness of any information, apparatus, product, or process disclosed, or represents that its use would not infringe privately owned rights. Reference herein to any specific commercial product, process, or service by its trade name, trademark, manufacturer, or otherwise, does not necessarily constitute or imply its endorsement, recommendation, or favoring by the United States Government or any agency thereof, or the Regents of the University of California. The views and opinions of authors expressed herein do not necessarily state or reflect those of the United States Government or any agency thereof or the Regents of the University of California.

Energy Conversion and Storage Program 1989 Annual Report

Elton J. Cairns, *Program Leader*

Applied Science Division
Lawrence Berkeley Laboratory
University of California
Berkeley, California 94720
(415) 486-5001

LBL-28737

LAWRENCE BERKELEY LABORATORY
APPLIED SCIENCE DIVISION

DIVISION DIRECTOR
EJ CAIRNS

DIVISION ADMINISTRATOR
CA FRAGIADAKIS

DEPUTY DIVISION DIRECTOR
DF GRETHER

ASSISTANT DIVISION DIRECTOR
AT QUINTANILHA

DIVISION COUNCIL
EJ CAIRNS, Chairperson

PROFESSIONAL STAFF COMMITTEE
MA WAHLIG, Chairperson

CENTER FOR ATMOSPHERIC AND BIOSPHERIC EFFECTS OF TECHNOLOGY
AT QUINTANILHA, Director

CENTER FOR BUILDING SCIENCE
AH ROSENFELD, Director

ENERGY CONVERSION & STORAGE PROGRAM
EJ CAIRNS, Leader
HW BLANCH, Deputy
MA WAHLIG, Deputy

- **ELECTROCHEMICAL GROUP**
  EJ CAIRNS, Leader
  FR MCLARNON, Deputy
  K KINOSHITA
- **MICROSTRUCTURED MATERIALS GROUP**
  AJ HUNT, Leader
- **BIOTECHNOLOGY**
  HW BLANCH
  CJ KING
  CR WILKE
- **FOSSIL FUELS**
  RH FISH
  S LYNN
- **HIGH T_c SUPERCONDUCTOR PROCESSING**
  PH BERDAHL
  AJ HUNT
  MD RUBIN
  RE RUSSO

ENVIRONMENTAL RESEARCH PROGRAM
T NOVAKOV, Leader
NJ BROWN, Deputy

- **ATMOSPHERIC AEROSOL GROUP**
  T NOVAKOV, Leader
  AD HANSEN
  WH BENNER
- **COMBUSTION GROUP**
  NJ BROWN, Leader
  RK CHENG
  D LUCAS
  AK OPPENHEIM
  RF SAWYER
  L TALBOT
  RB WILLIAMSON
- **MEMBRANE BIOENERGETICS GROUP**
  L PACKER, Leader
  RJ MEHLHORN
  AT QUINTANILHA
- **FLUE GAS CHEMISTRY GROUP**
  SG CHANG, Leader
- **ECOLOGICAL SYSTEMS**
  J HARTE
  SL ANDERSON
- **ANALYTICAL CHEMISTRY**
  F ASARO
  RD GIAUQUE

INDOOR ENVIRONMENT PROGRAM
JM DAISEY, Leader
AV NERO, Deputy

- **INDOOR RADON GROUP**
  WJ FISK, Acting Leader
  RG SEXTRO
  AJ GADGIL
- **INDOOR ORGANIC CHEMISTRY GROUP**
  JM DAISEY, Leader
- **INDOOR AIR QUALITY STUDIES**
  WJ FISK
  GW TRAYNOR
  - VENTILATION
  - CONTROLS
  - EXPOSURE ASSESSMENT
- **ENERGY PERFORMANCE OF BUILDINGS GROUP**
  MH SHERMAN, Leader

ENERGY ANALYSIS PROGRAM
MD LEVINE, Leader
RL RITSCHARD, Deputy

- **ENERGY CONSERVATION POLICY GROUP**
  MD LEVINE, Acting Leader
  JE MCMAHON
  AK MEIER
  I TURIEL
- **BUILDING ENERGY ANALYSIS GROUP**
  RL RITSCHARD, Leader
  H AKBARI
- **INTERNATIONAL ENERGY STUDIES GROUP**
  L SCHIPPER, Co-Leader
  JA SATHAYE, Co-Leader
  AN KETOFF
- **BUILDING ENERGY DATA GROUP**
  JP HARRIS, Leader
- **UTILITY PLANNING & POLICY GROUP**
  EP KAHN, Leader
- **GLOBAL ENERGY/ ENVIRONMENTAL ISSUES**
  MD LEVINE
  WE WESTMAN

BUILDING ENERGY SYSTEMS PROGRAM
MA WAHLIG, Leader

- **BUILDING SYSTEMS ANALYSIS GROUP**
  RC KAMMERUD, Leader
  WL CARROLL
- **SIMULATION RESEARCH GROUP**
  FC WINKELMANN, Leader
- **ABSORPTION HEAT PUMPS**
  JE RASSON
  MA WAHLIG

WINDOWS & LIGHTING PROGRAM
SE SELKOWITZ, Leader

- **WINDOWS & DAYLIGHTING GROUP**
  SE SELKOWITZ, Leader
  JH KLEMS, Deputy
  MD RUBIN, Deputy
  CM LAMPERT
  - OPTICAL MATERIALS
  - FENESTRATION PERFORMANCE
  - BUILDING APPLICATIONS
- **LIGHTING SYSTEMS RESEARCH GROUP**
  SM BERMAN, Leader
  RR VERDERBER, Deputy
  DD HOLLISTER
  DJ LEVY
  - LAMP TECHNOLOGY
  - IMPACTS
  - LIGHTING CONTROLS

April 1990

Energy Conversion and Storage Program Staff

Elton J. Cairns,* *Program Leader*
Harvey W. Blanch, *Deputy Program Leader*
Michael A. Wahlig, *Deputy Program Leader*

Thomas Adler
Daniel Arenson
Eduardo Baralt
Paul Berdahl
Rosemary Bittman
Harvey Blanch
Garth Burns
Van Carey
Wing-Tat Chan
Hung-Tse Chang
Douglas Clark
Thomas Colson
Louise Creagh
Dorys Rojas de Olivares†
Michael Dixon
Erik Fernandez
Richard Fish
Albert Flounders
Raymond Fong
Alan Foss
Hubert Gasteiger
Terry Grant
Cornelius Gross†
Gregory Hiller
Richard Hix
Arlon Hunt*
Benjamin Irvin†
Mark Isaacson
Jeffrey Kahn
Hyun-Ok Kim
Jung Wha Kim
Judson King III
Kimio Kinoshita
Judith Klinman
Mark Konings
Peter Kuhn†
Susan Lauer
Kevin Lofftus
Scott Lynn
Anthony Mancuso
Frank McLarnon‡
Jeffrey McMillan
Kenneth Miller
Stuart Naftel
Jon Noring
Loree Poole
Michael Prince
Lucy Randel
Bruce Rauhe
Ronald Reade
Marie Christine Richard†
Paul Ridgway
James Rudnicki
James Russell
Richard Russo
David Schurig
Robert Selleck
Mark Shannon
Daniel Shapiro
Susan Sharfstein
Jonathan Spear
Charlotte Standish
John Starr
Craig Stevens
Janet Tamada
Jerome Thomas
Jeffrey Weaver
Charles Wilke
Lamar Williams
Richard Williams
William Yang

*Group Leader
†Participating Guest
‡Deputy Group Leader

Contents

INTRODUCTION i

ELECTROCHEMICAL ENERGY STORAGE AND CONVERSION

Technology Base Research Project for Electrochemical Energy Storage 1
A Mathematical Model of the Rechargeable Zn/NiOOH Cell 3
In Situ Characterization of Zinc Electrode Processes 3
Extending the Lifetime of Zinc/Nickel Oxide Cells 4
Mathematical Modeling of the Sodium/Sulfur Cell 5
Evaluation of Sodium/Sulfur-Phosphorus Cells 5
Application of Photothermal Deflection Spectroscopy to Characterize Direct Methanol Electrooxidation 6
Characterization of Direct Methanol Electrooxidation 6
Evaluation of Direct Methanol Fuel-Cell Anode Performance 7

MICROSTRUCTURED MATERIALS

Microstructured Materials 8
Direct Solar Thermal Conversion 9
Optical Measurements of the Intracellular Polymerization of HbS 11
Modeling Biological Particles to Predict Optical Properties of the Ocean 11

BIOTECHNOLOGY

Transport and Physiological Studies of Hybridoma Metabolism 12
Separations by Reversible Chemical Complexation 16

FOSSIL FUELS

Removal of H_2S from Coal-Derived Gases 17
Bonding Studies of Nitrogen Heterocyclic Ligands to (η^5-Cyclopentadienyl)ruthenium Cation: A Novel Nitrogen-to-π Rearrangement 18
Hydroxylation of C_2, C_3, and CycloC_6 Hydrocarbons by Manganese Porphyrin and Non-Porphyrin Catalysts 19
A Functional Model for Methane Monooxygenase Enzyme: Hydroxylation of C_1-C_3 and CycloC_6 Hydrocarbons with Biomimetic Fe Cluster Catalysts in the Presence of Hydrogen Peroxide 18
Homogeneous Catalytic Hydrogenation of Aromatic Hydrocarbons and Heteroaromatic Nitrogen Compounds: Synthetic and Mechanistic Aspects 19

HIGH-TEMPERATURE SUPERCONDUCTOR PROCESSING

High-Temperature Superconducting Films: Electrical Characterization 20
Pulsed Laser Deposition as a Technique for Producing High-Temperature Superconducting Thin Films 21
Repetitively Pulsed Laser-Material Interaction and Steady-State Laser Sampling 22
High-Temperature Superconducting Thin Films Produced by Sputtering 24
Ultrasensitive Thermal Lens Spectroscopy 25

Introduction

The Energy Conversion and Storage Program applies chemical and chemical engineering principles to solve problems in 1) production of new synthetic fuels, 2) development of high-performance rechargeable batteries and fuel cells, 3) development of advanced thermochemical processes for energy storage, 4) characterization of complex chemical processes, and 4) the application of novel materials for energy conversion and transmission. Projects focus on transport-process principles, chemical kinetics, thermodynamics, separation processes, organic and physical chemistry, and advanced methods of analysis.

The electrochemical energy storage and conversion project develops advanced power systems for electric vehicle and stationary energy storage applications. Topics include identification of new electrochemical couples for advanced rechargeable batteries, improvements in battery and fuel-cell materials, and establishment of engineering principles applicable to electrochemical energy storage and conversion. Major emphasis is on applied research that will lead to superior performance and lower life-cycle costs.

Research in thermochemical energy storage and conversion focuses on new and innovative approaches using thermal and solar energy more efficiently. Gas-particle suspensions are being developed for use in direct solar-thermal conversion processes and for catalysis of important thermochemical reactions.

Coal-related research strives to develop improved, energy-efficient methods for processing waste streams from synfuel plants and coal gasifiers. Of particular interest are new techniques for removing compounds such as H_2S, NH_3, and phenols from effluents.

Energy-related chemistry projects seek to identify and characterize the constituents of liquid fuel-system streams and to devise energy-efficient means for their separation. Also of current interest is the development of advanced methods for producing alcohols from hydrocarbon fuels; the application of novel microstructured materials to develop super-insulating windows, new ceramics, and high-temperature superconducting films; use of ultrasensitive optical techniques to characterize dilute aqueous solutions; and the application of laser ablation to prepare high-temperature superconducting thin films.

— *Electrochemical Energy Storage and Conversion* —

Technology Base Research Project for Electrochemical Energy Storage

E.J. Cairns, K. Kinoshita, and F.R. McLarnon

LBL is the lead center for managing the Technology Base Research (TBR) Project, which is sponsored by the Electrochemical Branch of DOE's Office of Energy Storage and Distribution. This project's research supports DOE development of electrochemical energy conversion systems for electric vehicles and for stationary energy-storage applications. The project identifies promising electrochemical technologies and transfers these to industry and/or to other DOE programs for further development and scale-up.

The TBR Project identifies new electrochemical couples for advanced batteries, determines the technical feasibility of the new couples, improves battery components and materials, establishes engineering principles applicable to electrochemical energy storage and conversion, and investigates fuel-cell and metal/air systems for transportation applications. Major emphasis is given to applied research that will lead to superior performance and lower life-cycle costs.

LBL scientists participating in the project are E.J. Cairns, K. Kinoshita, and F.R. McLarnon of the Applied Science Division; and L.C. DeJonghe, J.W. Evans, R.H. Muller, J.S. Newman, P.N. Ross, and C.W. Tobias of the Materials and Chemical Sciences Division.

Research projects conducted by subcontractors are described in the report, *Technology Base Research Project for Electrochemical Energy Storage* (LBL-27037); in-house work is summarized in the next article and in the *Materials and Chemical Sciences Division 1989 Annual Report* (LBL-28100). Highlights of subcontracted work follow.

EXPLORATORY RESEARCH

Argonne National Laboratory (ANL) has continued its work on two advanced high-temperature rechargeable battery systems: 1) $LiAl/FeS_2$ cells containing a dense upper-plateau (U.P.) FeS_2 electrode, a Li-Al electrode, and LiCl-LiBr-KBr electrolyte (m.p. 310°C); and 2) $Na/\beta''\text{-}Al_2O_3/NaAlCl_4/NiCl_2$ cells ($Na/NiCl_2$ cells). An improved electrolyte-starved $LiAl/FeS_2$ cell with high performance (i.e., within 90% of that for flooded-electrolyte cells) and with a cycle life of >100 cycles was demonstrated. The performance of Ni electrodes in $Na/NiCl_2$ cells was enhanced in the presence of a small amount of sulfur, which appeared to decrease electrode impedance and increase porosity.

Projects are underway at the University of Pennsylvania and at SRI International to develop rechargeable conducting-polymer cells. The Univsersity of Pennsylvania is collaborating with the Energy Research Laboratory in Denmark to determine the factors that influence lithium-electrode cycle life in cells with conducting-polymer electrolyte. SRI International is synthesizing novel conducting polymers with sulfur and nitrogen atoms (instead of oxygen atoms) in the polyether chain structure, in order to improve the mechanical and electronic properties of the polymer. The University of Minnesota has completed its project on characterizing thin-layer electrochemical cells containing poly(ethylene oxide).

APPLIED RESEARCH

Stanford University has investigated the feasibility of liquid $NaI.4.5NH_3$ as a replacement for $\beta''\text{-}Al_2O_3$ solid electrolyte in Na/metal chloride cells. The transition-metal halides ($FeCl_2$, $NiCl_2$, and $CuCl_2$) were found to form insoluble reaction products in $NaI{\cdot}4.5NH_3$ at room temperature; practical use of this liquid electrolyte will therefore require use of a mixed-conductor matrix as an electrode structure.

The Massachusetts Institute of Technology completed its studies on fast-ion-conducting glasses for solid electrolytes in rechargeable Li/S cells. The addition of CaO to lithium borate glasses was shown to enhance chemical stability to lithium whereas it reduced ionic conductivity. To compensate for the latter effect of CaO, LiCl was added to increase the ionic conductivity .

The Illinois Institute of Technology (IIT) has successfully electrodeposited Mo and Mo_2C layers from a FLINAK (LiF-NaF-KF) melt. Experiments indicated that electrodeposition was mass-transfer controlled.

Brookhaven National Laboratory (BNL) and IIT have been studying the electrodeposition of Zn in electrolytes for flow batteries. BNL's EXAFS (Extended X-ray Absorption Fine Structure) studies of supersaturated zincate solutions have revealed evidence for the association of waters of hydration with $Zn(OH)_4$ ions. Having completed its studies of Zn electrodeposition from acidic $ZnBr_2$ electrolytes, IIT scientists have observed that application of pulse current produces a finer-grain deposit than that obtained at constant current.

Spectroscopic techniques (e.g., Raman, XPS, thermal desorption) are being applied at Case Western Reserve University (CWRU) and at Jackson State University to characterize the surface of reactive alkali and Zn electrodes in organic electrolytes and in KOH electrolytes. XPS studies showed that tetrahydrofuran reacts with lithium. Raman spectroscopy of Zn in KOH indicated that Zn^{2+} complexes with OH^-

Johns Hopkins University observed that 1018 carbon steel was susceptible to localized corrosion by pitting in both 0.5 M $LiClO_4$ and 0.5 M $LiAsF_6$ in highly purified propylene carbonate (PC) at potentials above the oxidation potential of PC.

AIR SYSTEMS RESEARCH

Research at CWRU has shown that heat treatment of the pyrochlore-based electrocatalyst, $Pb_2Ru_2O_{6.5}$, improves its corrosion resistance in bifunctional air electrodes. Further improvement has been obtained by depositing an anion-exchange membrane on the electrolyte side of the electrode in order to retard the transport of soluble Pb and Ru species from the porous electrode structure.

Research has been initiated at Metal Air Technology Systems International (MATSI) to investigate an LBL concept of reticulated metal structures for Zn electrodes in Zn/air cells. MATSI has shown that these structures can be extensively cycled (more than 100 Zn deposition/dissolution cycles) with Zn loadings of >100 mAh/cm^2.

Completed experiments at Pinnacle Research Institute have shown that Zn dendrites produced on a Mg substrate in a charge cell can be successfully discharged in a fluidized-bed slurry Zn/air cell.

SRI International's work on corrosion of Al in KOH electrolyte has been completed. Investigations of solution-phase inhibitors (e.g., Bi, Ga, In, Mn, Sn) have shown that these inhibitors deposit on the Al surface to reduce corrosion; this finding indicates that high-purity Al anodes may not be required in Al/air cells.

Los Alamos National Laboratory has been investigating the critical issue of water management in proton-exchange membrane (PEM) fuel cells. Measurements indicate that water transport by proton carriers through the cell is strongly dependent on the characteristics of the ionomeric membrane. When Nafion 117 (DuPont) is used, 2.5-2.9 H_2O molecules/H^+ ion are transported through the cell, whereas the value corresponding to use of a DOW membrane (Dow Chemical) is 1.5-1.8 H_2O molecules/H^+. The reduced water transport obtained with the DOW membrane indicates that use of this membrane will simplify water management in PEM fuel cells.

BNL's EXAFS studies of underpotential-deposited (UPD) Pb on Pt indicated a metallic-like character for the UPD layer as well as a shift of the absorption edge to higher energy.

Advanced Electrode Research

We have been studying the behavior of electrodes used in the advanced secondary batteries and fuel cells currently under development for energy-storage applications. In addition, we have been investigating practical means for improving the performance and lifetimes of these batteries and fuel cells. Systems of current interest include ambient-temperature, alkaline-electrolyte rechargeable cells with Zn electrodes (Zn/air, Zn/NiOOH); rechargeable high-temperature cells (Li/S, LiAl/FeS_2, Na/S and Na/$NiCl_2$); and fuel cells. We study life-limiting and performance-limiting phenomena under realistic operating conditions for the cell.

Alkaline Zinc Electrodes

Rechargeable alkaline Zn/air and Zn/NiOOH cells can be designed to deliver high specific energy and specific power, but these cells typically have short lifetimes. The high solubility of Zn species in alkaline electrolytes tends to enhance the physicochemical processes (e.g., active material redistribution and filamentary Zn growths) that degrade the cell's capacity and that limit its life. Through modeling and experimental investigations, we have been studying the complex transport processes involved in operating Zn electrodes. We have also been trying to characterize methods of reducing Zn species solubility and extending the lifetime of the Zn electrode.

A Mathematical Model of the Rechargeable Zn/NiOOH Cell

K.G. Miller, E.J. Cairns, and F.R. McLarnon

We have fully implemented a one-dimensional, time-dependent model of the Zn/NiOOH cell. This model, designed to elucidate the cause of active material redistribution in the Zn electrode, takes into account the transport of electrolyte species, heterogeneous chemical reactions, kinetics, and local variations in current density. The model has simulated 20-50 deep-discharge cycles to study the effects of different processes on the rate and extent of Zn redistribution.

Our simulations have provided useful insight into the effects of non-uniform current distribution. When current density at the top edge of the electrode is approximately 10% greater than the average value, the Zn material at the top of the electrode moves at a faster rate and exhibits a stronger spatial variation than is the case at the central region of the electrode. As the cell is cycled, the region of Zn material non-uniformity slowly extends to the lower portion of the electrode, although the rate of change here is slower than at the top of the electrode. In addition, the non-uniform distribution of current density results in steeper concentration gradients; diffusion and migration processes therefore become particularly important near the top edge of the electrode. Species movement through the separator is significantly more rapid than in the direction parallel to the plane of the separator. However, in areas of higher current density, the transport rate may not be high enough to replenish the reacting species, and this phenomenon can cause the concentration polarization. Results of our modeling show strong dependence on the value of the rate constants used for the ZnO chemical dissolution/precipitation reactions.

In Situ Characterization of Zinc Electrode Processes

J. Weaver, E.J. Cairns, and F.R. McLarnon

In our research directed at characterizing zinc electrodes, we have been using optical probe-beam deflection as an *in situ* technique to measure electrolyte concentration gradients in a model pore electrode. The model pore-electrode system, amenable to microscopic and spectroscopic study, is being used to simulate a real pore existing in the electrode of a rechargeable zinc battery. Conventional light microscopy is being used to observe surface species that form on the electrodes. The optical properties of the electrolyte are also being measured so that data on probe-beam deflection can be compared quantitatively to a one-dimensional numerical model of the transport processes in the model pore.

In order to study a continuous range of cell dimensions, we have improved the optical probe-beam deflection apparatus used to observe the concentration gradients. This improvement was accomplished by using a submicrometer-precision translation stage to control the height of the electrolyte compartment, which corresponds to the pore diameter; spacers of known thickness were not necessary to set the cell dimensions. The mounting and control system has been entirely rebuilt to closer tolerances, allowing our most recent experimental data to be more consistent than previously.

The new apparatus has been used to conduct several constant-current experiments. The resulting probe-beam deflection data were converted to refractive index gradients parallel to and perpendicular to the plane of the electrode surface. As expected, the parallel gradients were strongest near the mouth of the pore electrode—i.e., the side nearest the counter electrode. The direction of these gradients, as well as their relative magnitudes, had been predicted by the numerical model of the transient diffusion processes in this system. We have been refining this model to incorporate more accurate values of the electrolyte's optical properties.

The refractive index gradients normal to the electrode surface have also been measured. The steady-state values of these gradients provided a profile of the current density along the electrode surface. When incorporated into the numerical model, the profile provided good agreement between the experimental results and the model.

Attempts to induce precipitation of solid zinc species (a process known to occur in actual pores) in the electrolyte have been successful only at current densities much higher than those anticipated in a rechargeable zinc cell discharged at modest rates. Attempts to induce the precipitation included use of nylon diffusion barriers between the electrodes and as well as use of NiOOH counter electrodes. We have monitored precipitation by using optical microscopy and are now conducting precipitation studies that use scattering of the optical probe beam.

Extending the Lifetime of Zinc/Nickel Oxide Cells

T.C. Adler, F.R. McLarnon, and E.J. Cairns

Cycle-life performance of the Zn/KOH/NiOOH cell is seriously degraded by active material redistribution (shape change) of the Zn electrode, which results from migration of Zn across the face of the negative electrode and to the positive electrode. The process can be retarded by twofold reductions in electrolyte alkalinity, with a consequent fourfold reduction in zincate solubility. Alternate anions can be substituted for hydroxyl ions in order to maintain adequate ionic conductivity in these modified electrolytes. When carbonate and fluoride anions are used, cell-cycle life is triple that achieved when standard 6.8 M KOH/0.6 M LiOH electrolyte is used.

In 1989, several cells using reduced-alkalinity electrolytes approached or exceeded a goal of more than 300 cycles while maintaining more than 60% of initial capacity.

A test cell containing 2.5 M KOH/2.5 M K_2CO_3/0.5 M LiOH electrolyte reached 334 cycles. *In situ* x rays showed that the Zn electrode remained quite uniform at the end of life. Dendritic shorting incidence was only about half that seen in standard cells.

We have evaluated a wide range of alkaline-carbonate concentrations. At the low end of the range, a 2.5 M KOH/1.0 M K_2CO_3/0.5 M LiOH cell reached 175 cycles. A cell containing 6.8 M KOH/1.75 M K_2CO_3/0.5 M LiOH electrolyte reached 300 cycles at 63% capacity, indicating that even a low concentration of carbonate added to the standard electrolyte dramatically improves the cell's lifetime. An alkaline-fluoride cell (3.5 M KOH/3.3 M KF electrolyte) achieved 400 cycles at >70% capacity with only modest zinc redistribution.

Another approach to slowing zinc redistribution is to reduce zincate solubility by complexing it with $Ca(OH)_2$. Cells constructed with electrodes of 25 mole % calcium perform well in standard electrolyte; however, attempts to cycle these cells in alkaline-carbonate or alkaline-fluoride electrolytes have generally been unsuccessful. The failure of calcium-containing electrodes to form efficiently in these electrolytes probably results from preferential formation of $CaCO_3$ or CaF_2 instead of $CaZn(OH)_6$.

We have begun work on developing sealed cells. We are preparing cell cases with pressure-transducer attachments and have adapted the computer-controlled cell cycling system to monitoring pressures. Early sealed-cell experiments show that the Zn electrode is producing small but significant amounts of H_2; new electrode formulations are being investigated to suppress this unwanted phenomenon.

High-Temperature Cells

The high-temperature Na/S cell offers very good performance, and results of the recent improved process for manufacturing the ceramic β″ Al_2O_3 electrolytes indicate that acceptable cell lifetimes may be realized. However, the performance of the sulfur electrode has not been optimized, and the phenomena which govern its operation are poorly understood. In addition, Na/S cells cannot tolerate overcharge and overdischarge, a problem that complicates the design of cell-string configurations for battery applications. We are attempting to develop and confirm an advanced mathematical model of the sulfur electrode as well as to explore variants of Na/S cells that may exhibit improved performance and active material utilization.

Mathematical Modeling of the Sodium/Sulfur Cell

S.A. Naftel, F.R. McLarnon, and E.J. Cairns

We have developed a comprehensive model of the sulfur electrode in Na/S cells. The tubular central-sodium cell being modeled includes a thin layer of α-Al_2O_3 felt around the β″-Al_2O_3 solid electrolyte in order to prevent deposition of sulfur on the solid electrolyte during cell charge. The model consists of a set of non-linear PDEs describing the processes of diffusion, migration, and convection that take place during operation of such a cell. We have linearized these highly nonlinear equations and their boundary conditions by implementing a symbolic-equations manipulator written in the *Mathematica* computer program. *Mathematica* automatically generates the corresponding banded matrices used in the ADI-Newman technique for solving time-dependent PDEs. This work reduces tremendously the tedious effort necessary to linearize the PDEs and to generate the corresponding matrices necessary for numerical solution. The linearized equations are solved using a digital computer via implementation of the Newman-IAD method, a finite-difference technique for solving second- order linear PDEs.

Because of the mathematical complexity of the system—which involves simultaneous solution of elliptic and parabolic equations, the character (elliptic or parabolic) at each point dependent upon the phases present—the numerical solution has been split into two stages: 1) solution of the system in the one-phase region, and 2) solution of the system in the two-phase region. At present, our effort is directed toward (1), with work on (2) planned for the future. Significant results are expected during 1990. We will attempt to predict the effect of various charge-discharge regimens on cell operation.

Evaluation of Sodium/Sulfur-Phosphorus Cells

P.L. Ridgway, F.R. McLarnon, and E.J. Cairns

Addition of phosphorus to the sulfur cathode in the Na/S cell may improve power output by reducing resistance to sodium-ion transport. We anticipate that the long-chain sodium polysulfides that form in standard sulfur electrodes during discharge will be modified to lower-molecular-weight species by phosphorus, which may act as a molecular chain terminator in this system. By decreasing the viscosity in the cathode melt, this modification would allow faster transport of sodium ions in the melt, thereby decreasing the cell's overpotential and increasing its power output.

An initial melting-point study has indicated that, in general, the Na-P-S system has a higher melting point than expected. Thus, we are developing an experimental cell which will permit evaluation of optimal P/S ratios via equilibrium EMF measurements at temperatures up to 500°C. The cell uses β″-Al_2O_3 electrolyte and is constructed much like standard Na/S cells. Phosphorus/sulfur ratios which the EMF studies show to be promising will be tested in a practical Na/S cell configuration, and performance will be compared with that of standard Na/S cells.

Fuel Cells

Fuel cells can be designed to exhibit acceptable lifetimes for a number of applications. Our program is particularly interested in the use of fuel cells for transportation purposes. The performance of the O_2 electrode in fuel cells requires improvement, and development of an efficient direct-methanol fuel cell would represent a major advance over reformed-hydrocarbon fuel cells.

Application of Photothermal Deflection Spectroscopy to Characterize Direct Methanol Electrooxidation

J.D. Rudnicki, F.R. McLarnon, and E.J. Cairns

Photothermal deflection spectroscopy (PDS) is being used to study reactions at electrochemical interfaces. PDS is a sensitive in situ technique that measures the absorption spectrum of an electrochemical interface. This information helps to identify the reaction intermediates, which in turn help to determine the pathway by which the reaction occurs. PDS also measures the electrolyte concentration gradients adjacent to the electrode surface. These gradients contain information about the diffusion of reactants and products to and from the electrode. The sensitivity of these measurement techniques is high enough to detect reactions involving a single molecular layer of species on the electrode surface.

We have developed mathematical models of the chemical and physical processes occurring at the electrode surface. These models allow us to analyze the complex interaction of parameters governing the PDS system. The models have resulted in a more quantitative understanding of the PDS system.

We have also developed a method of measuring infrared absorption. The major difficulty encountered during prior optical investigations using this region of the spectrum involved the use of water-based electrolytes (nearly opaque in the infrared region) in many electrochemical systems of interest. Aided by mathematical models, we have designed a new cell that uses only a thin layer of electrolyte and allows the PDS system to obtain infrared spectra. Preliminary experiments have been successful. Future experiments will measure the spectrum of the species on Pt electrodes during the electrooxidation of CH_3OH.

Characterization of Direct Methanol Electrooxidation

H. Gasteiger, F.R. McLarnon, and E.J. Cairns

Fuel cells based on the direct electrooxidation of methanol promise an efficient, environmentally sound alternative source of power for vehicles. Unfortunately, the anodic reaction on Pt electrodes exhibits a large overpotential attributable to poorly understood poisoning reactions and rendering the above application economically unattractive.

A significant enhancement of the reaction rate has been observed on electrodes containing Pt-Ru alloy, and the quantitative characterization of this enhancement is the subject of our research. We have designed and are building an all-Teflon™ cell that will allow assessment of the rate of CH_3OH electrooxidation in HF and H_2SO_4 electrolytes at temperatures up to 100°C. Indications of preferential dissolution of Ru from these electrodes suggest that the alloy's surface—as distinct from its bulk composition—should be investigated in order to guarantee meaningful comparisons of catalyst (electrode) activities; auger electron spectroscopy will assist in this investigation. In addition, evaluation of the real catalyst surface area will be an important task not as easily carried out on Pt-Ru as on Pt alone. In combination with the electrochemical evaluations mentioned above, photothermal deflection spectroscopy will be used to elucidate the mechanisms of CH_3OH electrooxidation reactions, thereby providing a means for the "intelligent" design of more efficient catalysts.

Evaluation of Direct Methanol Fuel Cell Anode Performance

B. Rauhe, F.R. McLarnon, and E.J. Cairns

Methanol has gained much attention as a potential fuel for many fuel-cell applications. Ease of storage and distribution, wide availability, and low cost make methanol an attractive alternative to gaseous H_2; moreover, direct use of methanol as a fuel eliminates the need for bulky, expensive reformers that catalytically generate H_2 (for use as fuel) from a CH_3OH feed. We have been investigating and characterizing the performance of porous anodes as well as assessing the roles of several physical and chemical parameters. These parameters include electrode pore size and distribution; type, size, and distribution of catalyst (especially bimetallic catalysts); and electrolyte composition. Typically, the preferred catalyst is Pt supported on a carbon/Teflon™ structure. Prior investigations of combined catalysts such as Pt/Ru or Pt/Sn have shown promising synergistic increases in performance. We plan to study these bimetallic catalyst combinations in conjunction with our concurrent PDS investigations. The work will also be aided by an empirical mathematical model that will be used to predict anode performance using appropriate physical and chemical parameters as well as to help guide the interpretation of experimental data.

References

McLarnon FR, Cairns EJ. Energy storage. In: *Annual Review of Energy*. Palo Alto, CA: Annual Reviews, Inc . 1989; B14:241-71.

Cairns EJ, McLarnon FR. Advanced power sources for electric vehicles and stationary energy storage systems. Paper No. 322. Presented at the 175th Meeting of the Electrochemical Society, Los Angeles, CA, 1989.

McLarnon FR, Cairns EJ, Ismail MI. Introduction. In: Ismail MI, ed. *Fundamentals, Electrolyzers, Batteries and Fuel Cells*. Part A in *Electrochemical Reactors: Their Science and Technology*. Amsterdam: Elsevier Scientific Publishing Co. 1989; 1-8.

Weaver J, McLarnon FR, Cairns EJ. Investigation of a zinc model pore electrode using photothermal deflection spectroscopy. Paper No. 19-05-08-K. Presented at the 40th Meeting of the International Society of Electrochemistry, Kyoto, Japan, 1989.

Adler TC, McLarnon FR, Cairns EJ. Improved cycle-life performance with alkaline-carbonate electrolytes in Zn/NiOOH cells. Paper No. 5. Presented at the 176th Meeting of the Electrochemical Society, Hollywood, FL, 1989.

Rudnicki JD, McLarnon FR, Cairns EJ. In situ characterization of electrode processes by photothermal deflection spectroscopy. In: Varma R, Selman JR. eds., *Techniques for Characterization of Electrodes and Electrochemical Processes*. New York: John Wiley and Sons, 1989.

Rudnicki JD, Russo RE, McLarnon FR, Cairns EJ. Photothermal deflection spectroscopy: An in situ technique for the investigation of electrochemical interfaces. Paper No. 543. Presented at the 175th Meeting of the Electrochemical Society, Los Angeles, CA, 1989.

— Microstructured Materials —

Microstructured Materials

A. Hunt, H. Chang, M. Dixon, L. Kim, and K. Lofftus

This research develops new porous microstructured materials. These sol-gel-derived materials are characterized by highly unusual properties that make them useful in many applications: silica aerogel for insulating windows and in other transparent applications; new precursors for high-temperature ceramic materials and composites; and new methods to make high-critical-temperature superconductors. The materials are prepared at room temperature using sol-gel processing and supercritical drying: liquid organometallic compounds are reacted to form particles that link together in a solvent to form a porous network called an alcogel, and the solvent is then removed from the alcogel by a solvent substitution and supercritical drying technique discovered at LBL. The result is a low-density, transparent or translucent porous solid called *aerogel*. Using different starting compounds, we have developed methods to produce several single- and mixed-metal oxide compositions of aerogel.

SILICA AEROGEL: A TRANSPARENT SUPERINSULATOR

We have developed silica aerogel as transparent superinsulation for high-thermal-performance applications (R-20 per inch). Research at LBL has overcome the three primary barriers to large-scale production of silica aerogel. A safer, more economical supercritical drying process using liquid CO_2 has been developed and patented, the clarity of aerogel has been improved, and methods have been developed for using non-toxic starting compounds in producing high-quality aerogel. Economic studies indicate that mass-produced aerogel will be a cost-effective insulator in transparent and non-transparent applications. Evacuated silica aerogel appears to be an ideal material for replacing the CFC-containing polyurethane foams currently used in refrigerator insulation. Aerogel exhibits three or more times the thermal resistance of current insulating foams, and its use can eliminate a major source of the CFCs responsible for atmospheric ozone depletion and global warming.

Transparent aerogel sheets as large as 12 in^2 have been prepared at LBL using a new autoclave built specifically for CO_2 substitution and supercritical drying. The aerogel sheets have been encapsulated between glass to demonstrate their use as a window. Aerogel has also been placed into flexible plastic and evacuated for use as lightweight, high-performance insulating panels. The most recent stage of this project involved transfer of the technology to private industry. Thermalux, L.P. (reorganized from Quantum Optics Inc.) in Richmond, California was established to commercialize the manufacture of aerogel products using the patented CO_2 substitution process.

DEVELOPMENT OF POROUS MICROMATERIALS

LBL research and development in the area of micromaterials has been yielding new methods for producing microporous materials and precursors based on sol-gel chemistry and supercritical solvent-extraction techniques. Low-density materials having controlled microporosity promise to be useful in such applications as new ceramic precursors, high-temperature insulation, porous materials for filters, and catalyst substrates. Production of new composite ceramics may become possible, owing to the significantly lower sintering temperatures of very fine-grained aerogels (i.e., compared with the sintering temperatures of conventional ceramic powders). Lower sintering temperatures reduce the tendency for components to react with each other.

Recent progress includes the development of methods to produce zirconia, alumina, mullite (an alumina-silica ceramic) and composites of mullite and silicon nitride. Aerogels of all these materials are transparent in thin layers. We have also developed new methods for controlling the rate of hydrolysis of the alkoxide precursors, and a number of new formulations were explored. Monolithic and powdered aerogels were produced in each of these compositions.

SOL-GEL PROCESSING FOR PRODUCING SUPERCONDUCTING CERAMIC FILMS

The goal of this research is to produce high-T_c superconducting films using sol-gel processing. The advantages of developing successful sol-gel processing methods for oxide superconductors include inexpensive fabrication, very fine grain size, preparation of the oxides at lower temperatures than currently used, and manufacturing flexibility for coating wires or tapes. Advantages of the fine microstructure include enhanced low-temperature sintering and possibilities for improved flux pinning.

A key problem in using sol-gel processing to prepare high T_c superconductors has been the insolubility of copper complexes. In 1989, we successfully overcame this

problem by developing a method for synthesizing copper-barium ethoxy ethoxides, which are soluble in ethoxy-ethanols. Mixtures of this copper-barium alkoxide with yttrium isopropoxide and certain higher alcohols have been hydrolyzed with both acid and base catalysis using a new method of controlled hydrolysis developed at LBL. This method results in a mixture of copper hydroxide, copper oxide, barium hydroxide, yttrium hydroxide, and a phase tentatively identified as $Ba_2Cu(OH)_6$. After drying and mixing, submicron-sized powders of these salts were thermally decomposed in wet-flowing oxygen to crystalline products at temperatures as low as 500°C. We have developed a modified coating process that has produced thin films of similar compounds.

Direct Solar Thermal Conversion Processes

A. Hunt, M. Halmann, and P. Kuhn

We have been exploring advanced concepts in the direct conversion of concentrated solar energy to thermal and chemical forms. The energy may be used to drive gas-turbine generators, to supply industrial process heat, to produce useful chemical reactions, or to convert solar energy to chemical forms suitable for storage or transport. Our current research explores two areas: high-temperature gas receivers used to generate electricity; and concentrated solar energy used to detoxify hazardous chemical wastes. The unifying theme is the absorption of concentrated solar energy by small particles and the conversion of this energy to other forms. The concept of a gas-particle suspension as a solar absorber was first demonstrated by LBL in 1982 and has laid the foundation for the current research activities.

DIRECT-ABSORPTION HIGH-TEMPERATURE GAS-PARTICLE RECEIVERS

This research is part of the multiyear program being conducted jointly by investigators in the United States, Germany, Switzerland, and Spain to develop a high-temperature gas receiver based on the direct absorption of concentrated sunlight by entrained, submicron-sized particles. The goal is to build and solar-test a Direct Absorption Particle Injection Receiver (DAPIR) in 1993. Preparation consists of a series of experiments to determine the critical parameters for a DAPIR that uses carbon particles as absorbers. The first experiment on radiantly heated gas-particle dynamics was completed at LBL; the second experiment will measure radiant losses from heated gas-particle suspensions and is being carried out in Stuttgart at DLR, the German aerospace establishment.

The third experiment is being prepared at LBL with the participation of staff from the Paul Scherrer Institute in Switzerland. The objective is to measure the effect of radiant flux on the oxidation rate of carbon particles as a function of temperature. The results will determine the maximum operating temperature for carbon-particle-based gas receivers and will provide information necessary for designing the DAPIR.

Two forms of entrained particle receivers have been proposed. The first, the Small Particle Heat Exchange Receiver (SPHER) was developed at LBL and uses a window to contain a pressurized gas-particle suspension. More recently, Bechtel Corporation has proposed the Particle Injection Receiver, which operates without a window and uses a secondary gas-to-gas heat exchanger. Advantages of these receivers include high efficiency, high output temperatures, and low cost. These receivers have been identified as being the most promising approach to high-temperature gas receivers.

In both approaches, the very small mass of carbon particles used to absorb the sunlight is oxidized at the operating temperature to leave a clear gas stream. Therefore, the operating temperature depends on the oxidation rate of the particles. In solar testing of the SPHER, we discovered that the carbon particles were apparently oxidized at significantly lower temperatures in concentrated solar flux than when tested under isothermal conditions in the laboratory. This discovery, in addition to making oxidation measurements mandatory, underscores the importance of understanding the more general problem of solar flux's effects on chemical reaction rates in solid-gas systems.

We plan to carry out the particle oxidation measurements using the 30-kW solar simulator operating at LBL. The simulator will be equipped with a reaction cell designed and built in Germany. The cell consists of a high-temperature cavity containing a fused silica spiral that carries the dilute gas-particle suspension through a region of intense simulated solar radiation. The cell is designed to maintain the spiral at high temperatures (up to 1050°C) with or without intense solar radiation. The oxidation rate of suspensions of a variety of carbon allotropes will be measured (the thermal oxidation rate of carbon varies by five orders of magnitude, depending on the allotrope). The temperature, residence time, and radiant flux will be varied to measure the effects of flux on the particle oxidation rates.

After the carbon oxidation experiment is completed, the equipment used will be available for a variety of photochemi-

cal experiments. The solar-simulator flux source, in combination with the reaction cell and associated equipment, offers a powerful and flexible system for investigating the effects of radiant flux on chemical reactions at high temperatures. In particular, the system may be used to study solar detoxification mechanisms and other high-temperature solid-gas reactions.

SOLAR PHOTOLYSIS OF HALOCARBONS IN GROUNDWATER

Hydrocarbons and halocarbons—groundwater contaminates commonly released from industrial and agricultural activity—are present at various DOE sites. Usual methods of water purification (e.g., disinfection by chlorination or ozonization) can produce more harmful halocarbon derivatives or are ineffective wken applied to chlorinated hydrocarbons. In contrast, concentrated sunlight is effective in the photocatalyzed oxidation of aliphatic and aromatic hydrocarbons. Contaminated groundwater may be treated by direct exposure to concentrated sunlight in the presence of particles that serve as photocatalytic agents.

Research carried out in 1989 explored the effects of concentrated sunlight on groundwater containing halocarbons. Decomposition of dichloromethane in dilute aqueous solutions, as well as decomposition of 1,2-dibromo-3-chloropropane (DBPC) in polluted well water, was carried out in illuminated suspensions of TiO_2 particles or TiO_2-coated silica gel. In a collaborative effort, the State of California Department of Health Services supplied and characterized samples of groundwater contaminated with DBPC. (DBPC had been used intensively in agriculture from 1955 to 1977 as a nematicide fumigant—Nemagon—until it was banned because of its toxicity, particularly its ability to induce male sterility.)

Experimental results indicated that exposure to a radiant flux of approximately 100 suns intensity in the presence of the TiO_2-coated silica caused an approximately sixfold reduction of DBPC concentration. Results of the dichloromethane treatment indicated substantial increase of chloride ions, and pH changes continued for about two hours.

These preliminary measurements indicate that concentrated sunlight can be effective in the photocatalyzed oxidation of aliphatic and aromatic hydrocarbons. However, further laboratory measurements are required to optimize the reactor design and to determine the best conditions and reaction efficiencies for prevalent contaminates. Accurate measurement of destruction efficiencies will help us establish the flow rates and times that will determine the cost effectiveness of solar detoxification.

Reference

Miller F. *Radiative Heat Transfer in a Flowing Gas-Particle Mixture.* Ph.D. Dissertation, Department of Mechanical Engineering, University of California, Berkeley, California, 1988.

Studies of Light Scattering

To study the interaction of light with microstructures, we have been carrying out basic experimental and analytical studies of light scattering. In addition to our scattering studies in solar thermal conversion and microstructured materials, we have also been investigating light scattering in the biological sciences. To measure the light scattering, we have been using an angular scanning polarization nephelometer—an instrument capable of measuring all 16 elements of the Mueller scattering matrix. Various elements of this matrix are used to determine specific properties of the scatterers.

Optical Measurements of the Intracellular Polymerization of HbS

A. Quintanilha, A. Hunt, H. Salamon, and R. Macey

We have been using a polarization-sensitive light-scattering technique to measure the kinetics of intracellular polymerization in sickle cell hemoglobin. The polymerization of hemoglobin S (HbS) in the red blood cells of individuals with sickle cell disease appears to be a major factor leading to capillary occlusion and crisis. Dehydration, deoxygenation, and increased acidification stimulate intracellular HbS polymerization, and because these processes occur in the kidney environment (the kidney is one of the organs most frequently damaged by sickle cell disease), we have simulated these conditions *in vitro* to study their effects on HbS polymerization. The polarization-sensitive light-scattering technique developed earlier was used to measure the degree of polymerization. The latter was measured by the S_{14} element of the scattering matrix.

Our results indicate that the amount of induced circular polarized light increases in the dehydrating hypertonic medium representative of the kidney environment. Furthermore, successive cycles of deoxygenation-reoxygenation appear to lead to progressively larger steady-state values of this component of the scattered light.

We have also observed that 1) the rates of polymerization and depolymerization as a function of changing oxygen tension are clearly different—the rate of polymerization is much slower than the rate of depolymerization; and 2) even the red cells from sickle-trait subjects, which contain significantly lower levels of HbS, show evidence of polymerization at low oxygen tensions and in hypertonic media. The first observation is important in determining whether the transit time of red cells through the kidney (approximately 24 seconds) is enough to allow polymerization of HbS. The second observation can probably be related to kidney function abnormalities that develop in sickle-trait patients.

We have conducted experiments to distinguish between the intracellular polymerization of HbS and the resulting changes of the cell shape. These experiments have indicated that other elements of the scattering matrix contain information about the shape changes but are unaffected by the polymerization. We have begun to design an advanced instrument that will offer greater flexibility and sensitivity for the measurements.

Modeling Biological Particles to Predict Optical Properties of the Ocean

A. Hunt, M. Quinby-Hunt, K. Lofftus, and D. Shapiro

We have been studying light scattering in the ocean by combining experimental and modeling techniques. In this work, the intensity and polarization of scattered light as a function of angle are used to investigate the nature of the particles and to predict the propagation of light in the ocean. Because the particle population in the ocean is often dominated by organisms with defined size, shape, and optical properties, light scattering can be used to investigate the presence of certain ensembles of organisms in the sea and to predict their effects on the optical properties of the ocean.

We have used a concentric-sphere model (based on the Mie theory) to determine the optical characteristics of marine *Chlorella*. We found that only a very restricted set of assumptions regarding the optical properties and dimensions of the

organism could provide simultaneous fitting of three elements of the scattering matrix to the experimental measurements. Cells of the dinoflagellate *Prorocentrum micans* were measured in solution and while immobilized in a transparent silica gel. Time-varying circular polarization signals were observed from solutions of *Prorocentrum mican*. Very strong signals were also observed from the immobilized cells. We are working to interpret these data from a structural and biological viewpoint.

References

Hunt AJ, Lofftus KL, Quintanilha A. Optical measurements of the intracellular polymerization of HbS. *Blood* 1987;70:62a.

Quinby-Hunt MS, Hunt AJ, Lofftus KD, Shapiro D. Polarized light studies of marine chlorella. (*Limnology and Oceanography*, in press, 1989)

Lofftus, KD, Quinby MS, Hunt AJ, Livolant F, Maestre M. Light scattering by prorocentrum micans: A new method and results. (*Applied Optics*, in press, 1989)

— *Biotechnology* —

Transport and Physiological Studies of Hybridoma Metabolism

Harvey W. Blanch, Douglas S. Clark

MITOCHONDRIAL HEXOKINASE ACTIVITY IN A MURINE HYBRIDOMA

Hybridomas, like most transformed cells, exhibit high rates of aerobic glycolysis. Glucose is converted to lactate at very high yields (typically 1 to 2 moles/mole), resulting in a loss of most of the available energy. Recent studies of glucose catabolism indicate that high rates of aerobic glycolysis are not related to abnormal pyruvate oxidation via the tricarboxylic acid cycle (TCA) or abnormal oxidative phosphorylation. Rather, high aerobic glycolytic rates are believed to be the result of a breakdown of glycolytic regulation. Abnormal hexokinase and pyruvate kinase activities (when compared to activities of cells grown *in vivo*) are believed to be responsible for poor glycolytic control in many transformed cells. Pyruvate kinase in transformed cells has been found to have a decreased apparent affinity for its substrate which results in a "bottleneck" in glycolysis at the level of phosophoenolpyruvate (PEP). This "bottleneck" leads to an accumulation of many glycolytic intermediates, including fructose-1,6-diphosphate (F-1,6-DP) and eventually to a breakdown in regulatory control of phosphofructokinase. Normally, phosphofructokinase is inhibited by ATP levels in the cytosol. Glycolytic rates are thus kept in balance with rates of pyruvate utilization (i.e. ATP formation) in the TCA cycle. However, very high levels of F-1,6-DP overcome the inhibitory effect of ATP whereby phosphofructokinase regulation is lost. Accumulation of F-1,6-DP also leads to an accumulation of fructose-6-phosphate (F-6-P) and glucose-6-phosphate (G-6-P). Thus, in order for glycolysis to proceed at a rapid rate, hexokinase activity must not be inhibited by the accumulation of glucose-6-phosphate.

In most mammalian tissues, the primary regulators of hexokinase are G-6-P and glucose-1,6-diphosphate (G-1,6-DP). Hexokinases bound to the outer membrane of mitochondria have been found to exhibit high levels of specific activity and not to be strongly inhibited by G-6-P. In our work, we present evidence for the presence of a mitochondrially bound hexokinase in a murine hybridoma and some preliminary findings of its regulation.

Hexokinase Distribution and Kinetic Parameters

The mitochondrial fraction was found to contain 25 ± 2% of the total hexokinase activity for both methods of cell disruption. The effect of glucose and ATP concentration on the rate of glucose phosphorylation was examined for both the cytosolic and the mitochondrial enzymes.

Linear least-squares regression analyses were used to calculate values for K_m. For the cytosolic enzyme, the K_m values for glucose and ATP are 0.23 and 0.38 mM, respectively. For the mitochondria-bound enzyme, the corresponding values were very similar; the K_m for glucose was 0.26 mM and was 0.44 mM for ATP. To verify that the hexokinase activity associated with the mitochondrial fraction remained attached to the membrane during the assay procedure, this fraction was recentrifuged at 20,000 × g for 10 minutes. Virtually all hexokinase activity was found in the pellet, indicating that the enzyme was associated with the mitochondrial membrane during assay. The glucose K_m for the cytosolic and mitochondrial enzymes are very similar; therefore, for X-D hybridomas, high fluxes through hexokinase are not the result of high substrate affinities for the mitochondrial enzyme (relative to the cytosolic enzyme).

Hexokinase regulation

The cytosolic hexokinase is much more strongly inhibited by G-6-P than is the mitochondrial hexokinase. Activity is inhibited 50% at low concentration for the cytosolic enzyme (0.07 mM), whereas only a 38% drop in activity was observed for the mitochondrial enzyme at the highest concentration tested, 4.4 mM.

A NUCLEAR MAGNETIC RESONANCE TECHNIQUE FOR DETERMINING CELL CONCENTRATION IN HYBRIDOMA HOLLOW-FIBER CULTURE

Hollow-fiber bioreactors have proven useful for cultivating many mammalian cell types at high cell concentrations. High fiber loadings provide large mass-transfer areas, which are essential for conducting metabolic studies at tissue-like cell concentrations. Hollow-fiber reactors have also been used in nuclear magnetic resonance (NMR) spectroscopic studies of intracellular processes. Because NMR is a relatively insensitive analytical technique, high cell concentrations are needed to obtain quantifiable signals in a reasonable amount of time (< 1 hour).

One problem encountered when using hollow-fiber reactors is inaccurate determination of cell concentrations in the extracapillary space. This information is essential for expressing metabolic rates on a per-cell or per-cell-volume basis. Because drawing representative samples regularly from the ports of the reactor is not possible without causing a substantial upset of the culture, noninvasive techniques must be used.

The most common noninvasive method for determining cell concentrations in mammalian-cell hollow fiber culture is to make estimates based on rates of nutrient uptake. However, such estimates rely on the assumption that the consumption rate of a metabolite per cell (specific consumption rate) is constant. This assumption may be true over a limited range of environmental conditions but is of little utility when conditions are changed dramatically. For example, a frequently used parameter used for cell mass estimates is *rate of oxygen uptake.* The specific oxygen consumption rate for a murine hybridoma has been found to vary moderately (<40%) for large changes in glucose, glutamine, lactate and ammonia concentrations in continuous suspension culture.

In this work, we describe a ^{23}Na-NMR method for determining the cell concentration within a hollow fiber bioreactor. Because the intracellular concentration of sodium is low (approximately 7mM for hybridomas), and the extracellular concentration is very high (100 to 150 mM in most media), the total sodium content of the reactor decreases as the cell concentration increases. By monitoring the change in the total sodium level detected with ^{23}Na NMR, we are able to monitor changes in cell mass. Changes in intracellular sodium levels are likely to be small and their effects on cell volume measurements are essentially negligible, as described below.

A typical ^{23}Na spectrum (Figure 1) was acquired by using 90° pulses, a 205-ms acquisition time, and essentially no relaxation delay; 5-Hz line-broadening was used for signal-to-noise enhancement. Because sodium has a large quadrupole magnetic moment, it relaxes very rapidly. Thus, nuclei for the resonances shown were fully relaxed between pulses. The signal-to-noise ratio for the reactor resonance in the 21-second acquisition shown in Figure 1 was 440:1. The

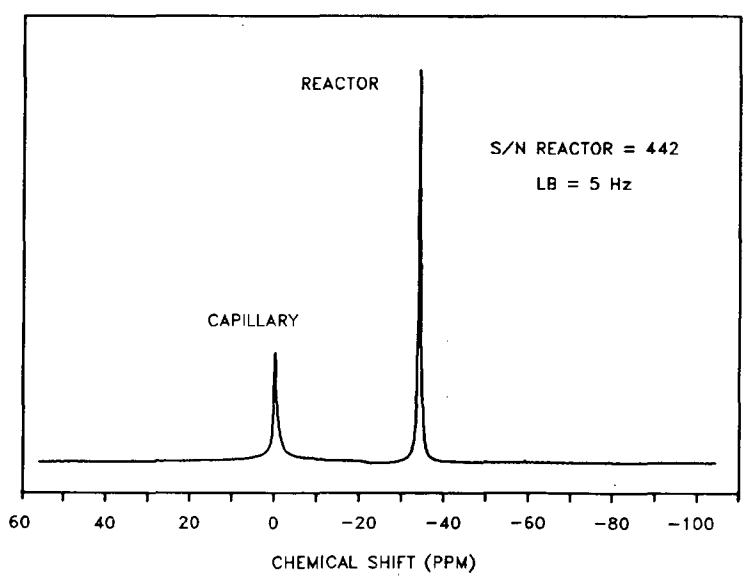

Figure 1. Typical Sodium spectrum with resonances for reactor and capillary. Spectra (2K points) were collected at 47.637 MHz with 90° pulses and a 205-ms acquisition time. No recycle delay was used. The spectrum was collected with 100 scans; total acquisition time, 21 seconds.

reactor signal includes contributions from both intra- and extracellular sodium and decreases with time as cell mass accumulates in the reactor.

For a typical spectrum of ^{31}P metabolites (Figure 2), detectable resonances include the internal standard MDPA, sugar phosphates, NTP (which has three resonances, one for each phosphate), phosphodiesters (PDE), phosphoenolpyruvate (PEP), and inorganic phosphate (P_i), which contains both intra- and extracellular contributions. The β-NTP resonance, which is unique to triphosphates and contains no contribution from NDP or NMP, was used to quantify total intracellular NTP. This spectrum was acquired in 15 minutes by using 70° pulses, a 205-millisecond acquisition time, and a relaxation delay of 800 milliseconds; 20-Hz line-broadening was used to enhance the signal-to-noise ratio, which was 12:1 on the β-NTP resonance. This spectrum was acquired when the culture in the reactor had grown to saturation. During the initial stages of growth, longer acquisition times (as long as 3 hours) were needed to obtain adequate signal-to-noise ratios for quantitation.

The precision of the ^{23}Na cell volume determinations can be estimated from the error in the NMR measurements. Each data point shown in Figure 3 represents the average of four independent 21-second acquisitions. The standard deviation for the cell fraction estimate was <2% when the cell concentration was highest (>180 hours). The standard deviation was much higher for measurements made at lower cell concentrations (<60 hours), because of the difficulty in accurately determining a small difference between two large numbers.

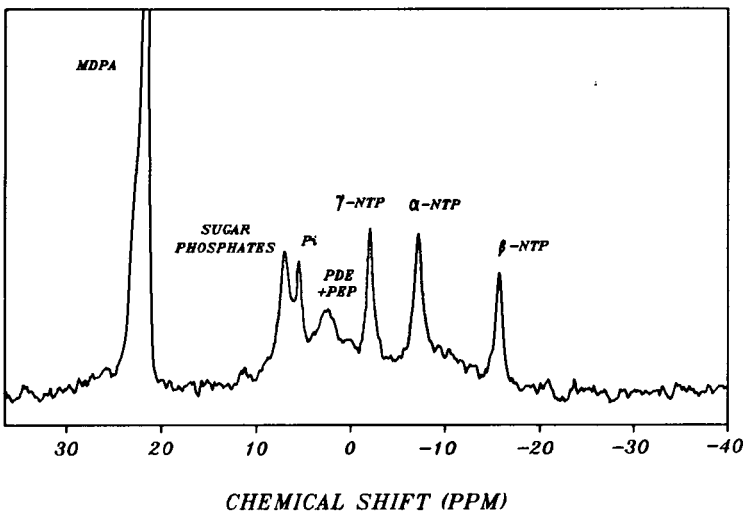

Figure 2. Typical 31p spectrum with a 15-minute acquisition time.

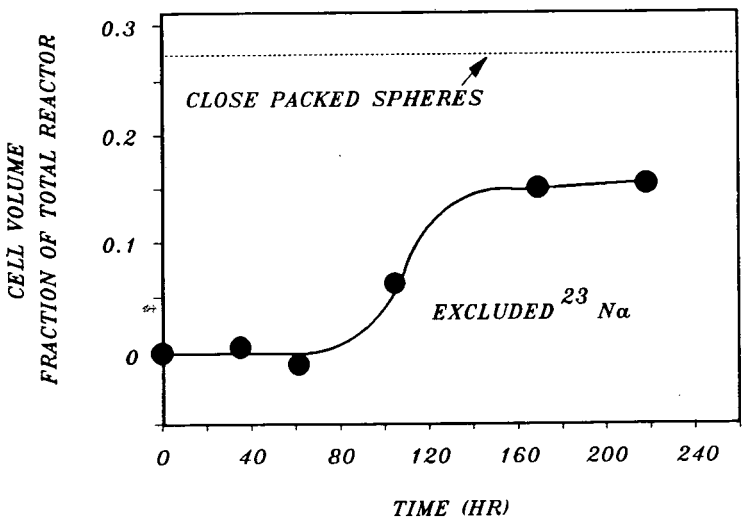

Figure 3. Time course of total excluded ^{23}Na within the reactor in hollow-fiber culture. Each data point represents the average of four 21-second measurements.

The time course of NTP and oxygen utilization for the same experiment is shown (Figure 4). Both profiles quantitatively follow the same pattern. The fact that both data sets so closely parallel each other supports the hypothesis that they both indicate cell mass. The ^{23}Na measurements qualitatively follow the same pattern, although the ^{23}Na measurements are not sensitive enough to detect the initial increase during the first 60 hours.

To assess the accuracy of our ^{23}Na cell-mass determinations, we estimated the reactor cell concentration at the end of the experiment for all three types of measurements described above. For these estimates, the average cell diameter in the reactor was assumed to be 15 microns (based on measurements made from light micrographs of stationary-phase cells in flask culture) and that the specific oxygen consumption rate was 0.27 mmol/10^9 cell-hr (observed for X-D cells grown in suspension culture at a low dilution rate (0.4 day^{-1}). The results of these calculations are summarized below.

Cells/ml	Method
~9.4 x 10^7	Excluded Na
~1.2 x 10^8	Total NTP
~9.1 x 10^7	Oxygen Consumption

These estimates indicate that the cell concentration in the reactor is about 1 x 10^8 cell/ml. The approximate agreement between the different methods is encouraging and suggests that ^{23}Na measurements are fairly accurate. In a previous report, we estimated the cell concentration for another hybridoma line grown in a similar hollow fiber unit to be 1 x 10^8 cells/ml. Other researchers have found similar hybridoma concentrations (in hollow-fiber reactors) ranging from 4 x 10^7 to 2 x 10^8 cells/ml.

Our estimates of cell number indicate total cytoplasmic volume in the reactor. Because the rate of antibody synthesis is believed to be governed by rate of mRNA translation and rate of excretion through the Golgi apparatus, this is a suitable approximation. If the rate of antibody synthesis is governed by the rate of transcription of heavy- and light-chain DNA, the utility of our results would be diminished—estimates of the number of nuclei would be a much more desirable result. However, current research indicates that cytoplasmic phenomena are rate-limiting.

References

Fernandez EJ, Mancuso A, Murphy MK, Blanch HW, Clark DS. Nuclear magnetic resonance methods for observing intracelular environment of mammalian cells. *Annals of the New York Academy of Sciences* (in press, 1990).

Miller WM, Wilke CR, Blanch HW. Transient responses of hybridoma cells to lactate and ammonia pulse and step changes in continuous culture. *Bioprocess Engineering* 1988; 3:113-122.

Miller WM, Wilke CR, Blanch HW. Transient responses of hybridoma cells to nutrient additions in continuous culture: I. Glucose pulse and step changes; and II. Glutamine pulse and step changes. *Biotechnology and Bioengineering* 1989; 33:477-486.

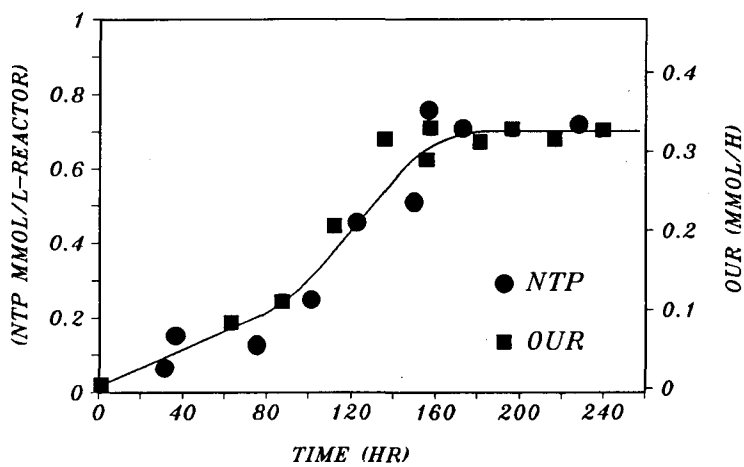

Figure 4. Time course of total reactor NTP and oxygen utilization rate in hollow-fiber culture.

Separations by Reversible Chemical Complexation

C.J. King, D.R. Arenson, L.J. Poole, L. Randel, J.N. Starr, J.A. Tamada, and L. Vingerhoet

Reversible chemical complexation is a potentially attractive method for recovering carboxylic acids, alcohols, glycols, and related substances from the dilute and complex solutions that result from manufacture from biomass by fermentation. Our work has focused on implementing complexation through extraction and sorption processes.

The presence of co-extracted water considerably increases the solubilities of carboxylic acids in certain organic solvents. This phenomenon forms the basis for a novel regeneration process in which co-extracted water is removed from the extract by stripping and in which the carboxylic acid product is simultaneously recovered by precipitation.

The solubility of fumaric acid in methyl isobutyl ketone (MiBK) increases fivefold in the presence of water. Positive effects of co-extracted water on fumaric acid solubility have also been found with n-octanol, n-butyl acetate, di-n-butyl ether, tributyl phosphate, and Alamine 336 in either MiBK or toluene. Co-extracted water also increases the solubilities of succinic and adipic acids in MiBK.

Another promising method of regeneration uses back-extraction of a carboxylic acid from an organic-phase extract (e.g., Alamine 336—a high-molecular-weight tertiary amine—in an organic diluent) into an aqueous solution of a low-molecular-weight tertiary amine (e.g., trimethylamine, TMA). The resultant aqueous solution is concentrated by evaporation, and the trialkylammonium carboxylate is decomposed thermally, yielding the volatile tertiary amine (for recycling), as well as the carboxylic acid product. The high-molecular-weight amine has very low solubility in water, whereas the low-molecular-weight amine has high aqueous solubility.

Experimental results for back-extraction of lactic, fumaric, and succinic acids from Alamine 336/MiBK extracts into aqueous TMA solutions have shown that essentially all the TMA pairs with carboxylic acid, even if this leaves little carboxylic acid in the organic phase. Furthermore, partitioning of TMA into the organic phase is very low as long as substantial stoichiometric excess of TMA does not remain. Results of the back-extraction agree with a predictive model based upon measured values of K_d for the forward extraction and literature data for the pKa of TMA and of the carboxylic acids.

In the cases of fumaric and succinic acids, crystals of the acid form in a viscous solution when water and TMA are evaporated. When this mixture is redissolved in MiBK and reevaporated, more than 80% of the carboxylic acid is recovered as crystals. Because of its much higher solubility in water, lactic acid does not form crystals and yields only a glassy mass containing TMA.

Borates form complexes reversibly with cis-diols. Because of differing stability constants, complexation with borates affords a way to fractionate among glycol isomers. The pH value is important because the boronate ion—not the free boronic acid—forms the complex. The pK_a of boric acid is 9.2; therefore, boric acid forms complexes with diols only at pH above 8. For recovery of glycols from solutions of neutral or lower pH, a boronic acid with higher acidity is needed.

3-Nitrophenylboronic acid (NPBA) has a pK_a near 7 and forms complexes with diols at pH values as low as 5. We have determined that the solubility of NPBA in water is 0.40 wt%. We have also measured stability constants for 1,2-propanediol with 3-nitrophenylboronic acid.

— *Fossil Fuels* —

Removal of H_2S from Coal-Derived Gases

S. Lynn, T. Colson, R. Hix, and C. Stevens

As coal becomes gasified, most of its sulfur is converted to H_2S and must be removed before the gas can be used either as a fuel or as synthesis gas. The UCB Sulfur Recovery Process (UCBSRP) is being developed as a general method for removing H_2S from gases. The H_2S is absorbed in a polyglycol ether and then caused to react in the liquid phase with SO_2 to form marketable elemental sulfur and water. The process allows high specificity and flexibility: H_2S can be reduced to the part-per-million level (or lower) in the presence of CO_2 and other components of gasified coal. The CO_2 may be left in the original gas stream or it may be co-absorbed and recovered as a separate, sulfur-free product. The process thus has application both for syngas and hydrogen production from O_2-blown gasifiers and for power production using an air-blown gasifier.

SULFUR CRYSTALLIZATION

A major potential advantage of the UCBSRP is the purity of the crystalline sulfur produced. The sulfur crystallizes from solution, both as a result of cooling and as a result of chemical reaction between H_2S and SO_2. Experiments using thermal crystallization have indicated that the mixed-suspension, classified-product-removal (MSCPR) model can be used to correlate the data. Changes in residence time produce changes in nucleation and in growth through their common driving force, supersaturation. The effect of supersaturation manifests itself in the general slope of the curves when the data are plotted. Although the density of the slurry changes slightly with residence time for a MSCPR crystallizer, large changes in slurry density were made by altering the feed temperature in the second set of experiments.

The crystallization apparatus was used to perform the liquid-phase reaction of H_2S and SO_2 and the crystallization of sulfur in an integrated vessel. These experiments were done to demonstrate the feasibility of the reactor/crystallizer in the UCBSRP and to verify the reactor/crystallizer model being developed in parallel with the experimental program. High-quality rhombic sulfur crystals with a mass-average size of 250 microns or higher were produced in the laboratory experiments, and the model based on thermal crystallization adequately predicted the crystal-size distribution of the reaction product.

ABSORPTION WITH CHEMICAL REACTION

Data on tray efficiency are needed for two process situations. In one, H_2S at a very low concentration is absorbed by a chemically reactive solution of SO_2; in the other, gaseous SO_2 in the low parts-per-million concentration range is absorbed by lean process solvent. Both processes are of interest because stringent sulfur removal is intended with the UCBSRP. Equipment consisted of a single sieve tray (or section of packed column) placed in a test section through which pass streams of gas and liquid. Reactive-absorption rate data were collected at various temperatures and for various catalyst concentrations and H_2S feed rates. In a typical set of reactive-absorption experiments, the average second-order rate constant was 11.2 liter/mole-s at a catalyst concentration of 0.015 M 3-pyrridyl carbinol. This value compares favorably with the rate constant of 16.0 liter/mole-s measured at the same catalyst concentration by other investigators using an adiabatic batch reactor.

We have written a computer program that incorporates the Murphree vapor tray efficiencies of H_2S and SO_2 and the reaction between these two components to serve as a tool for absorber design. To allow design of high-pressure absorbers, we used a correlation (taken from the literature) that represented the ambient-pressure data well.

PROCESS CONFIGURATION STUDIES

Major goals of this project are 1) to demonstrate the feasibility of replacing conventional industrial gas treatment technology with the UCBSRP technology, and 2) to compare the costs of the UCBSRP with those of conventional processes. One promising application of the UCBSRP is for removal of H_2S and CO_2 from a synthesis gas after a water-gas shift reaction in a process for producing high-purity hydrogen.

Evaluation of the flowsheet for such a process yielded a maximum required H_2 sales price of about \$930/ton. This price would result in a three-year (before tax) payout of the capital investment and corresponds to a situation where the CO_2 has no recoverable value. Currently, refinery-grade H_2 (i.e., purity ≥90%) is valued at between \$360 and \$2900/ton, depending on purity and geographic location. Thus, the preliminary results of our process study indicate a potentially viable process. If the H_2 plant were constructed in a geographic area having a large market for CO_2, the process would become even more attractive.

Studies of Organometallic Synthesis and Catalysis

The Organometallic Chemistry Group focuses on two areas of research. The first area includes the bonding studies of polynuclear heteroaromatic nitrogen (PHN)—model coal compounds with organorhodium and organoruthenium complexes—and the chemistry associated with these nitrogen-bonded or π-bonded complexes. Homogeneous catalysis studies on regioselective hydrogenation of PHN compounds (using the abovementioned complexes as catalyst precursors) is an important goal of this program.

Our second area of research, biomimetic catalysis, is directed toward elucidating the synthesis and catalytic activity of mimics of methane monooxygenase enzymes. Conversion of small hydrocarbons (such as methane), to their respective alcohols (i.e., methanol), is the major goal of this project and includes the mechanistic aspects of these oxidation reactions.

Bonding Studies of Nitrogen Heterocyclic Ligands to (η^5–Cyclopentadienyl)ruthenium Cation: A Novel Nitrogen-to-π Rearrangement

R.H. Fish, H.S. Kim, and R.H. Fong

We reacted the nitrogen heterocyclic ligands-pyridine (**1**), 2-methylpyridine (**2**), 2,4-dimethylpyridine (**3**), 2,4,6-trimethylpyridine (**4**), quinoline (**5**), 2-methylquinoline (**6**), benzoate and substantiated its formation from CD_4. Other mechanistic aspects with complexes (**1**) and (**2**) were studied and included k_H/k_D ratios with cyclohexane that were found to be 1.96 and 2.25, respectively, whereas C_3/C_2 hydrogen selectivities (normalized) with adamantane were found to be 3.41 and 3.26, respectively. The UV-vis analysis of the reaction mixtures of **1** and **2** with hydrogen peroxide showed absorptions at 484 and 513 nm, values consistent with literature values for Fe peroxo complexes. Our results suggest that several possible intermediate oxidants could be involved in the C-H activation reaction and include both $Fe^{V}O$ or $Fe^{III}OO$ cluster complexes, but probably not a hydroxyl radical (HO·).

Hydroxylation of C_2, C_3, and Cyclo$_6$ Hydrocarbons by Manganese Porphyrin and Non-Porphyrin Catalysts

R.H. Fish, R.H. Fong, R.T. Price, J.B. Vincent, and G. Christou

Metal complexes that mimic the active site of monooxygenase enzymes and that convert carbon-hydrogen bonds to carbon-hydroxyl in the presence of a monooxygen transfer reagent are called *biomimetic catalysts*. To study the activation of methane, ethane, propane, and cyclohexane to their respective alcohols, we have used biomimetic catalysts that encompass manganese supramolecule porphyrins and open-faced porphyrins, manganese non-porphyrin tri- and tetranuclear clusters, and a mononuclear manganese-substituted Keggin ion in the presence of monooxygen transfer reagents such as iodosylbenzene and t-butyl hydroperoxide.

A Functional Model for Methane Monooxygenase Enzyme: Hydroxylation of C_1-C_3, and CycloC_6 Hydrocarbons with Biomimetic Fe Cluster Catalysts in the Presence of Hydrogen Peroxide

R.H. Fish, R.H. Fong, M.S. Konings, J.B. Vincent, and G. Christou

A functional biomimic for the methane monooxygenase enzymes, $Fe_2O(OAc)_2Cl_2(bipy)_2$, **(1)**, and its synthetic precursor, $[Fe_4O_2(OAc)_7(bipy)_2]ClO_4$, (2) have been found to activate C1-C3 and cycloC_6 hydrocarbons with the monooxygen transfer reagent, hydrogen peroxide, in acetonitrile. The methanol formed from methane with **(1)** and **(2)** as catalysts was verified by derivatization with benzoyl chloride in the presence of pyridine to provide methyl benzoate. A similar experiment with methane-d_4 (CD_4) clearly showed the formation of CD_3OH as methyl-d_3

Homogeneous Catalytic Hydrogenation of Aromatic Hydrocarbons and Heteroaromatic Nitrogen Compounds: Synthetic and Mechanistic Aspects

R.H. Fish

We have reviewed the synthetic and mechanistic aspects of the homogeneous catalytic hydrogenation of mono- and polynuclear aromatic hydrocarbons as well as the corresponding heteroaromatic nitrogen compounds. Considering both classes of compounds, we have compared regioselectivities under various hydrogenation conditions for a wide variety of transition-metal complexes with regard to substrate binding at the metal center, as well as the role of free-radical intermediates in metal carbonyl hydride reactions (in which the substrate does not bind to the metal center prior to hydrogen transfer). Under similar reaction conditions, the polynuclear heteroaromatic nitrogen compounds appear to hydrogenate more readily than do the polynuclear aromatic hydrocarbons. We have addressed the relative rates of hydrogenation of a variety of heteroaromatic nitrogen compounds as well as compounds that inhibit and enhance selective hydrogenation of the nitrogen-containing ring. A relatively new spectroscopic technique, high-pressure nuclear magnetic resonance spectroscopy, has been shown to be a powerful tool for elucidating the mechanisms of the regioselective hydrogenation of polynuclear heteroaromatic nitrogen compounds.

References

Fish RH, Kim HS, Fong RH. Bonding studies of nitrogen heterocyclic ligands to (η^5-cyclopentadienyl)ruthenium cation: A novel nitrogen to π rearrangement. *Organometallics* 1989; 8:1375.

Fish RH, Fong RH, Price RT, Vincent JB, Christou G. Hydroxylation of C_2, C_3, and CycloC_6 hydrocarbons by manganese porphyrin and non-porphyrin catalysts. *ACS Symposium Series* 1989: 392:116.

Fish RH. Homogeneous catalytic hydrogenation of aromatic hydrocarbons and heteroaromatic nitrogen compounds: Synthetic and mechanistic aspects. In: *Aspects of Homogeneous Catalysis*. Dordrecht, The Netherlands: Kluwer Academic Publisher (in press, 1990).

— *High-Temperature Superconductor Processing* —

High-Temperature Superconducting Films: Electrical Characterization

P. Berdahl, A. Meyers, T. Mosig, and J. McMillan

This project has been closely coordinated with research on synthesis of superconducting thin films by sputtering (M. Rubin), pulsed laser deposition (R. Russo), and sol-gel deposition (A. Hunt). The thin-film research is intended to lead to development of high-current thin films that can be incorporated into electrical conductors such as tapes or wires. Electrical characterization of these films is required to understand electrical losses and to determine the conditions under which full advantage of superconductivity can be maintained.

In this project, we hav been routinely measuring resistance versus temperature by using the standard four-point technique in a variable-temperature cryostat. The latter apparatus, developed specifically for our research, is automated and uses low-frequency (37 Hz) current excitation as well as a lock-in amplifier to determine the corresponding voltage drop. Cooling to 13°K is provided by a closed-cycle helium refrigerator. The dewar has a narrow tail that facilitates application of an external magnetic field to the sample. A Pt temperature sensor is used to minimize temperature errors induced by the magnetic field. The basic resistance measurement has sufficient sensitivity to follow the decreasing resistance upon cooling for 4 or 5 orders of magnitude below the typical film resistance of a few ohms.

Critical current density (J_c) is measured by increasing the current through the sample until a small, measurable voltage appears (~1 mV/cm). The apparatus used is the same as that used for resistivity measurements but with an amplifier to boost the applied current as necessary. Of the films we have fabricated and measured, the highest-quality film with highest transition temperature is laser-deposited epitaxial $YBa_2Cu_3O_7$ on strontium titanate, exhibiting a resistance of 0 at 91.6°K and a J_c which at 90°K rises above the contact resistance limit of 10^3 A/cm, even in a 0.4-tesla field. SQUID magnetization measurements show persistent circulating current values well above 10^5 A/cm^2 at 5°K; however, the primary emphasis of our research is to develop high-current films for metal tapes (i.e., not to achieve high-quality films on single-crystal substrates). The best films on metal substrates at present show sharp resistive transitions and exhibit J_c values on the order of 10^3 A/cm^2 at 77°K. These values decline sharply when a magnetic field is applied. These measurements show that the films on metal substrates perform as well as high-quality bulk ceramic materials but are currently unoriented, as characterized by electrical measurements and by x-ray diffraction; performance is expected to improve as we achieve additional orientation in the films.

Our most interesting electrical measurements to date are for a thin-film sample rotated in a fixed field of 0.4 tesla (Figure). For $\theta = 0$, the field is normal to the $YBaCu_3O_7$ film;

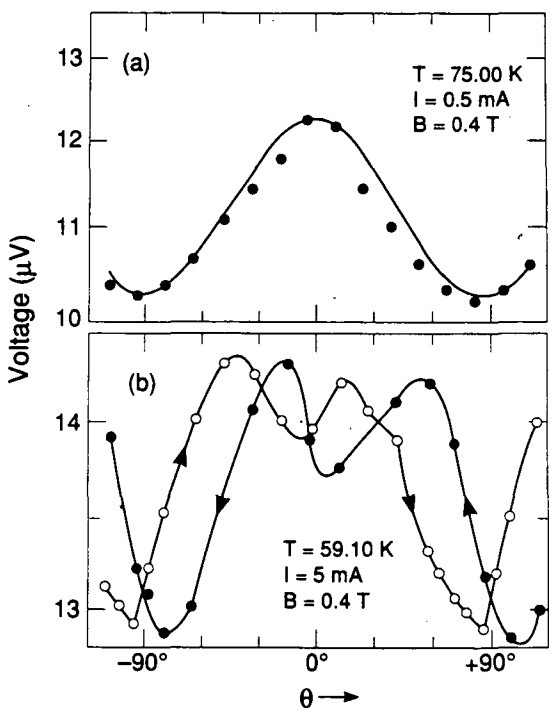

Figure. Voltage drop as a function of direction of an applied magnetic field. Points show measured data. Upper curve is a cosine function; lower curves are visual guides. (XBL 8910-6328)

at $\theta = 90°$, the field is parallel. In all orientations, the field is perpendicular to the transport current. At 75°K (upper part of Figure), the voltage drop (proportional to film resistance) shows a smooth, simple dependence on the magnetic field angle, θ, indicating that the anisotropic crystallites of which the film is composed tend to be aligned with the substrate. The simple function cos (2θ) approximates the data.

At lower temperatures, more complex and hysteretic behavior appears (lower part of Figure). (The two curves are for increasing and decreasing values of θ). Circulating supercurrents, induced by the change in field orientation relative to the film, evidently interact with the transport current to produce this complex pattern. The data demonstrate that Jc measurements performed in a magnetic field depend on details of how the field is applied.

We plan to continue routine and advanced transport measurements, focusing on the low-frequency, few-tesla, high-current range (relevant to electric power applications). Further experiments and computations are essential in order to attain a quantitative understanding of energy losses in superconductors. Such quantitative understanding can eventually form the basis for designing high-performance conductor structures.

Pulsed Laser Deposition as a Technique for Producing High-Temperature Superconducting Thin Films

*R.E. Russo, R.P. Reade, J. McMillan, B.L. Olsen**

To study and develop pulsed laser deposition for making thin-film high-temperature superconductors, we have constructed new pulsed laser deposition systems at the Lawrence Berkeley Laboratory (LBL) and at the Lawrence Livermore National Laboratory (LLNL). A new excimer laser used at LBL can provide 750 mJ per pulse at 248 nm, with a repetition rate of 100 Hz. The two laser deposition systems provide complimentary studies with different lasers and operating parameters. Both these systems provide the capability for depositing multi-layered thin-film conductors and for depositing films in the 700°C temperature range with high O_2 pressures. New Kanthal-filament heaters were developed for these conditions. A turret-type target holder was designed to rotate four bulk materials separately into the laser-beam path.

Using excimer-laser ablation, excellent as-deposited YBCO superconducting thin-films have been fabricated on $SrTiO_3$, MgO, and sapphire. We also developed the laser ablation technique for depositing uniform metal films of Ag, Au, and Pt on various substrates. YBCO films were laser deposited on metals and these metal films. Significant results were achieved for YBCO films deposited on Ag-film/stainless steel configurations. The R *vs* T curve for an as-deposited YBCO thin film on stainless steel with a silver buffer layer is shown (Figure).

Bi and Tl films were fabricated using the laser ablation approach. Rutherford backscattering spectroscopy (RBS) analysis indicated that the laser-deposited films contained the correct metal stoichiometry, although the films were not superconducting as deposited.

A new laser vaporization approach for making thin films was discovered in a collaborative effort with Professors Don Olander and Mehdi Balooch of the UC Berkeley Department of Engineering. A long-pulse (millisecond), 50 joule Nd:glass laser was employed for the vaporization studies. The first film was deposited on a quartz substrate, and its stoichiometry was measured using RBS. Film thickness was measured to be approximately 0.4 mm using only two laser pulses. RBS results indicated the stoichiometry to be $Y1Ba_{1.94}Cu_{3.22}O_{6.7}$. Based on this result, a second film was deposited on $SrTiO_3$ heated to 500°C. A reactive oxygen rf

*Chemistry and Materials Division, Lawrence Livermore National Laboratory.

plasma was incorporated in the chamber and was found to enhance the oxygen content during deposition. However, the as-deposited film was not superconducting because of low oxygen content, and it required post-deposition annealing. After a 0.5-h anneal at 850°C in oxygen, a resistive transition starting at 60°K was measured. This was the first high-temperature superconducting thin-film ever produced in several seconds using just two laser pulses. A second two-hour anneal of this film improved the transition to T_c onset at 80°K and T_c zero at approximately 63°K.

Potential advantages of this vaporization approach include fast deposition rates that lead to continuous coating of films on tapes, large-area deposition, and inexpensive initial capital costs. Our preliminary results have been submitted for publication, and a second manuscript is in preparation. In addition, DOE patent protection is being sought for this new vaporization technique.

We plan to continue studying and developing pulsed laser deposition for making as-deposited thin-film high-temperature superconductors. Research will continue in the area of multilayered thin-film configurations. This work will include the laser deposition of metal (Ag, Au) buffer layers and single-crystal materials ($SrTiO_3$, MgO) on practical substrates such as stainless steel. We also plan to investigate the laser deposition of metal and polymer films over the superconducting films to enhance their chemical stability. An increased effort is planned to fabricate as-deposited Bi thin films.

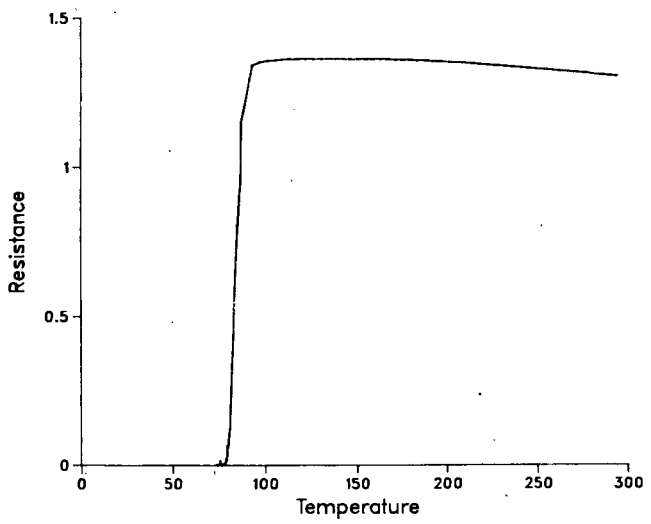

Figure. Resistance-versus-temperature curve for an as-deposited YBCO thin film on stainless stell with a silver buffer layer.
(XBL 902-621)

Repetitively Pulsed Laser Material Interaction an Steady-State Laser Sampling

R.E. Russo, W.T. Chan, and M. Shannon

This project, initiated in 1989, has been studying the fundamental mechanisms underlying the interaction of repetitively pulsed high-power lasers with condensed-phase materials. The laser-material interaction is not well understood; only approximate mechanisms based on vaporization (thermal) or ablation (shock-wave) processes have been proposed to describe this complex interaction. We proposed to study the laser-material interaction over a wide range of power densities using *in situ* techniques to probe the interaction region and using optical emission spectroscopy to characterize the sampled material.

In our research, repetitively-pulsed laser-sampled material is transported to an inductively coupled plasma (ICP). The ICP serves as the excitation source for steady-state atomic emission spectroscopy (AES) and as a real-time monitor of the laser-material interaction. ICP is an excellent excitation source because of its high temperature and ability to dissociate stable molecules or clusters that can form during the laser pulse. An available ICP has been aligned with a monochromator detection system, and an ablation chamber has been constructed.

Real-time *in situ* monitoring techniques are being investigated for studying the laser-material interaction. The techniques evaluated initially include acoustic (thermal expansion, shock wave) monitoring and optical probe-beam deflection (OPBD). Using a piezoelectric sensor attached to the material and/or a microphone enclosed in the surrounding chamber, the acoustic time and amplitude response are being studied for their ability to provide information on laser heating, the onset of explosion, and plasma formation. Changes in the acoustic response as a function of laser power will be correlated to changes in the material removal processes. The laser's power density can be increased from below the threshold of explosion to a level at which the plasma is produced. Initial research has identified wide-bandwidth PZTs and geometrical designs for observing acoustic wave propagation.

OPBD, which is based on the displacement of a probe laser-beam by refractive index gradients, is being developed to measure heating and cooling rates and to distinguish between heating and material-removal processes. Using a HeNe laser beam propagating adjacent and parallel to the material surface, a distinct change in the index of refraction (of the atmosphere above the material surface) is expected as the material is heated through its vaporization temperature. During the initial heating phase, the probe beam will be deflected away from the surface because of a lower local refractive index. However, as material vaporizes, the refractive index should increase because of a concentration gradient of atomic and molecular species above the surface. Therefore, the deflection response should show an abrupt change in direction at the onset of vaporization. An initial OPBD experimental arrangement has been developed, and preliminary results have indicated that geometric changes during a phase change (solid to liquid) impose severe signal limitations which distort information about the response of the heating mechanism.

Correlation of data from these *in situ* techniques with atomic emission in the ICP will be analyzed to enable better understanding and utilization of the repetitively pulsed laser-material interaction. Our 1990 research will expand on these initial studies, with the goal of understanding the fundamental mechanisms underlying removal of material during high-power laser impingement.

High-Temperature Superconducting Thin Films Produced by Sputtering

M. Rubin

This project uses a sputtering technique to make high-temperature superconducting thin films for use in electric power applications.

We have sputtered YBCO films onto single crystal substrates having high critical temperatures and currents as deposited. We then deposited similar films onto polycrystalline metal substrates with buffer layers of silver and strontium titanate. When grown on these substrates, the films remain superconducting while critical currents are reduced to bulk levels.

Diffusion of elements from the substrate was studied by Auger depth profiling, and measurements were made showing the effects of tensile strain on conductivity. We plan to continue to investigate the influence of ion bombardment on the growth temperature, microstructure, and other properties.

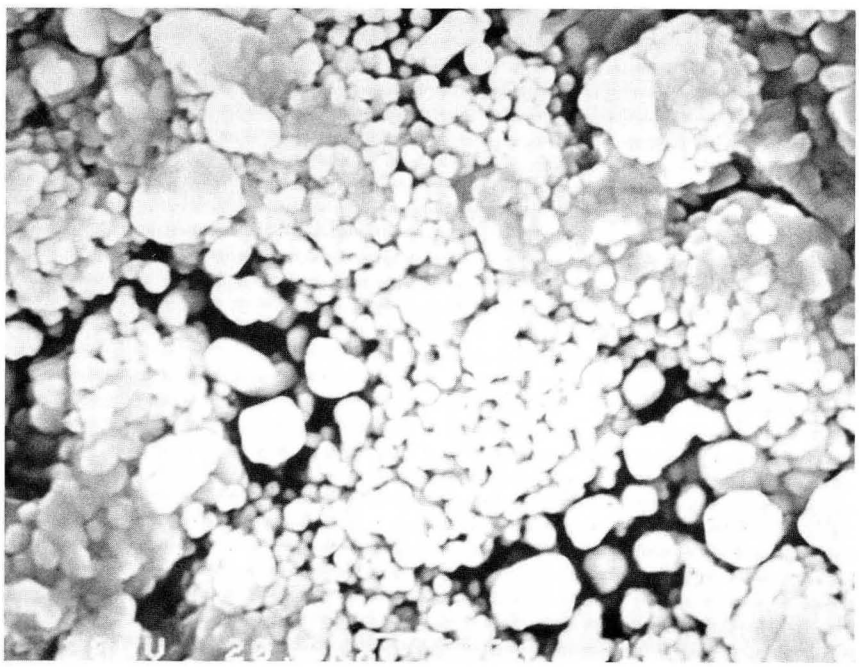

Figure. Photomicrograph shows cracking of YBCO film due to thermal-mismatch stress on a metal substrate.

Ultrasensitive Thermal Lens Spectroscopy

*R.E. Russo, J.D. Spear, R.J. Silva**

A dual-beam differential thermal lens spectrometer (TLS) was developed and employed for the ultrasensitive analysis of rare-earth and actinide species in aqueous solutions (Figure). A pulsed Nd:YAG laser beam induces a transient thermal gradient in the sample medium. With this Gaussian laser beam excitation (TEM_{200}), the heating is greatest in the center of the beam, and the induced refractive index gradient resembles a high-quality divergent lens (the optical path-length is shortest at the beam center). With the assumptions that the absorption coefficient (a) is small ($a < .01\ cm^{-1}$), and that all energy absorbed is converted to heat (no fluorescence), the steady-state focal length (f) of the induced lens is:

$$f = F(apkw^2, 2.303P(dn/dT)A) \tag{1}$$

where k is the thermal conductivity of the medium ($W\ cm^{-1}K^{-1}$), w is the laser beam spot size at the sample (cm), P is the laser power (W), A is the dimensionless absorbance (Beers Law) and (dn/dT) is the refractive index dependence on temperature (K^{-1}). The refractive index dependence on temperature is determined primarily by changes in the sample density. Most materials expand when heated, resulting in a negative value for (dn/dT).

A second paraxial probe laser was employed to probe the refractive index profile, and its defocusing was measured. The strength of the thermal lens was obtained by measuring the change in intensity at the probe-beam center using a pinhole (spatial filter) and photodetector. The change in measured intensity through the pinhole is directly proportional to the absorption in the sample. The change in laser intensity DI is:

$$F(DI, I) = F(-2.303P(dn/dT)A, lk) \tag{2}$$

where I is the intensity at the beam center and l is the wavelength (cm). A small intensity modulation is induced on the continuous probe laser beam by the modulated thermal lens, and detected by an boxcar integrator. Optical filters are employed to block the excitation beam so that only the probe laser is incident on the detector behind the pinhole.

The position of the induced thermal lens relative to the excitation beam waist (focal position) affects the laser beam diameter at the detector pinhole. For maximum sensitivity the sample is placed at the focal spot of the excitation laser beam and one confocal distance (Z_c) beyond the probe beam waist (w) where Z_c is:

$$Z_c = F(pw^2, l) \tag{3}$$

This dual-beam differential TLS system was employed for the measurement of rare-earth species in aqueous solutions with real-time background subtraction. Background refers to optical absorption by the solution, which must be subtracted from the total thermal lens signal to indicate actual absorption by the sample species. Using the developed system, we measured an absorbance sensitivity of $2.7 \times 10^{-7}\ cm^{-1}$ which is at least three orders of magnitude more sensitive than commercial spectrometers and an order of magnitude more sensitive than photoacoustic spectroscopy. The spectrometer will be utilized at LLNL for measurements of actinide speciation and complexation in various aqueous environments.

*Nuclear Chemistry Division, Lawrence Livermore National Laboratory.

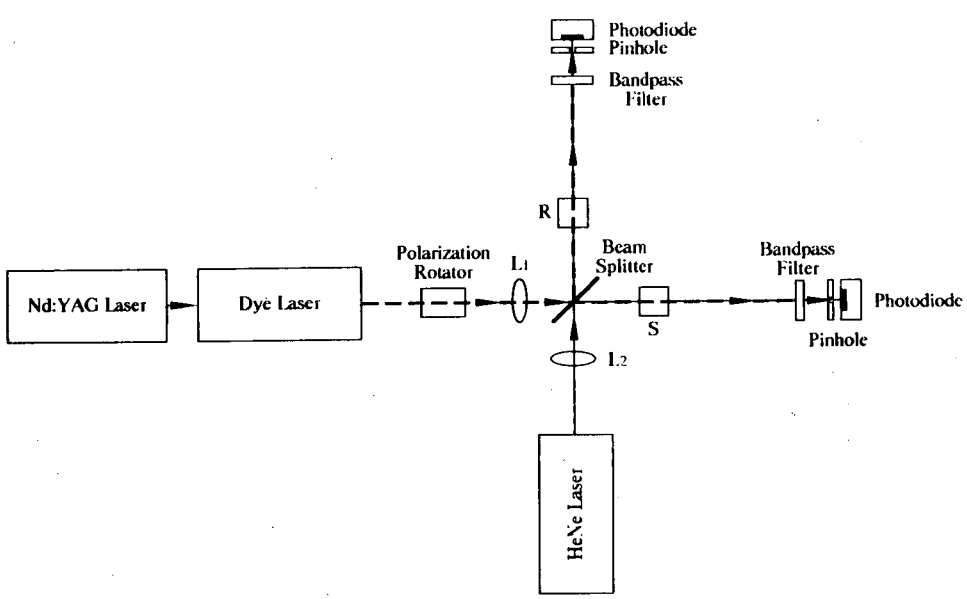

Figure. Schematic of dual-beam differential thermal lens spectrometer. (XBL 902-620)

Projects described in this report were supported by the following sources:

- Assistant Secretary for Conservation and Renewable Energy, Office of Energy Storage and Distribution, Energy Storage Division, U.S. Department of Energy
- Assistant Secretary for Conservation and Renewable Energy, Office of Energy Systems Research, Energy Conversion and Utilization Technologies (ECUT) Division, U.S. Department of Energy
- Assistant Secretary for Fossil Energy, Office of Coal Utilization, Division of Surface Coal Gasification, U.S. Department of Energy
- Director, Office of Energy Research, Office of Basic Energy Sciences, Chemical Sciences Division, U.S. Department of Energy
- Environmental Sciences Programs Directorate of the Office of Naval Research
- National Institutes of Health, National Heart, Lung and Blood Institute
- Electric Power Research Institute

This support was provided through the U.S. Department of Energy under Contract DE-AC03-76SF00098 and under Lawrence Livermore National Laboratory Contract No. W-7405-ENG-48.

DISCLAIMER

This document was prepared as an account of work sponsored by the United States Government. Neither the United States Government nor any agency thereof, nor The Regents of the University of California, nor any of their employees, makes any warranty, express or implied, or assumes any legal liability or responsibility for the accuracy, completeness, or usefulness of any information, apparatus, product, or process disclosed, or represents that its use would not infringe privately owned rights. Reference therein to any specific commercial product, process, or service by its trade name, trademark, manufacturer, or otherwise, does not necessarily constitute or imply its endorsement, recommendation, or favoring by the United States Government or any agency thereof, or The Regents of the University of California. The views and opinions of authors expressed herein do not necessarily state or reflect those of the United States Government or any agency thereof or The Regents of the University of California and shall not be used for advertising or product endorsement purposes.

Lawrence Berkeley Laboratory is an Equal Opportunity Employer

Applied Science Division
Lawrence Berkeley Laboratory
University of California
Berkeley, CA 94720